Glycobiology vol. 12 no. 4 pp. 241–250, 2002

Solution structure of two xenoantigens: αGal-LacNAc and αGal-Lewis X

Francisco Corzana[2,3], Emmanuel Bettler[2], Catherine Hervé du Penhoat[2], Tatyana V. Tyrtysh[4], Nicolai V. Bovin[4], and Anne Imberty[1,2]

[2]Centre de Recherche sur les Macromolécules Végétales (Affiliated with Joseph Fourier University), BP 53, F-38041 Grenoble cedex 9, France; [3]Departamento de Química, Universidad de La Rioja, Madre de Dios, 51, E-26006 Logroño (La Rioja), Spain; and [4]Shemyakin and Ovchinnikov Institute of Bioorganic Chemistry, Russian Academy of Sciences, ul Miklukho-Maklaya 16/10, 17871 GSP-7, V-437, Moscow, Russia

Received on June 19, 2001; revised on August 31, 2001; accepted on August 31, 2001

Organ hyperacute rejection, a phenomenon occurring during discordant xenotransplantation, is due to the recognition of an oligosaccharide epitope by human xenoreactive natural antibodies. In addition to the αGal(1-3)βGal(1-4)GlcNAc trisaccharide, a fucosylated structure, αGal-Lewis X, has been shown to be recognized by the antibodies. Both the trisaccharide and the tetrasaccharide have been synthesized by chemical methods. A complete nuclear magnetic resonance characterization of the two compounds has been performed, including the measurements of two-dimensional nuclear Overhauser effect spectroscopy data. Molecular dynamics simulations were run for several ns in the presence of explicit water molecules. The combination of experimental and theoretical approaches revealed the effect of an additional fucose residue on the conformational behavior of the xenoantigen. This branched fucose strongly rigidifies the N-acetyllactosamine. The effect on the αGal(1-3)Gal fragment is less marked. In the presence of fucose, the terminal αGal residue can still adopt two different conformations, but the equilibrium populations are modified.

Key words: /molecular dynamics/NMR/oligosaccharides/ xenotransplantation

Introduction

Xenotransplantation—grafting of an organ from another species, generally from pig to human—is considered to be the main potential remedy for the shortage of donor organs (see review by Auchincloss and Sachs, 1998). The first barrier to be overcomed for transplanting a pig organ into a human is the hyperacute vascular rejection that occurs in the first minute (Cascalho and Platt, 2001). The antigen responsible for this hyperacute vascular rejection has been identified as the linear B oligosaccharide αGal1-3βGal1-4βGlcNAc (Cooper *et al.*, 1993) that is present on the endothelium of all mammals, except in higher apes and man (Galili *et al.*, 1988; Oriol *et al.*, 1999). On the other hand, antibodies against this epitope are present in all humans and higher apes (Galili *et al.*, 1987; Samuelsson *et al.*, 1994). Recognition of the αGal epitope by these preformed antibodies activates both the pig cells and the human complement cascade, resulting in rapid thrombosis in the pig organ (Sandrin *et al.*, 1993).

Much effort has been devoted to the conformational analysis of the αGal1-3Gal disaccharide because this compound is the epitope recognized by human xenoreactive natural antibodies. In addition to an early nuclear magnetic resonance (NMR) study (Lemieux *et al.*, 1980), energy maps of this linkage have been calculated with the help of the MM2 (Strotz and Cerezo, 1994; Bizik and Tvaroska, 1995) or MM3 programs (Imberty *et al.*, 1995). Recently, the conformational study of an analogue, αGal1-3βGal1-4βGlc-1NAc, has been performed by a combination of Monte Carlo calculations and NMR spectroscopy (Li *et al.*, 1999). In all recent studies, the αGal1-3Gal epitope has been predicted to be rather flexible because it adopts at least two different conformations in solution.

In addition to the linear αGal1-3βGal1-4βGlcNAc epitope, present on glycolipids and glycoproteins of pig endothelial cells, a branched epitope, αGal1-3βGal1-4(αFuc1-3)βGlcNAc (αGal-Le^x) has been characterized as a component of glycosphingolipids expressed in pig kidney (Bouhours *et al.*, 1997, 1998). This tetrasaccharide has been revealed by immunostaining with a polyclonal antibody directed against αGal1-3Gal1 determinants. Schematic representation of the oligosaccharides are given in Scheme 1.

The present study is dedicated to the comparison of the solution conformational behavior of these two oligosaccharides in the aim of defining their common conformational epitope recognized by cross-reacting antibodies. Both the linear trisaccharide and the branched tetrasaccharide have been synthesized and fully characterized by NMR. The conformational behavior of both compounds has been determined by molecular dynamics simulations in explicit water environment. The calculations were validated by comparing theoretical and experimental nuclear Overhauser effect spectroscopy (NOESY) data.

Results

NMR data

Chemical shifts and coupling constants. The ^{1}H and ^{13}C assignments for **2** and **4** were based on 2D correlation spectra (see *Materials and methods*), and these data have been collected in Tables I and II, respectively. There is very good agreement between the chemical shifts of **2** and **4** and the ones previously obtained for related oligosaccharides. ^{1}H and ^{13}C chemical shifts have been reported for compounds similar to trisaccharides **1** and **2,** αGal1-3βGal-OR (where R = –$(CH_2)_8CO_2Me$; Lemieux *et al.*, 1980) and αGal1-3βGal1-4βGlc-Nac (i.e., with

[1]To whom correspondence should be addressed

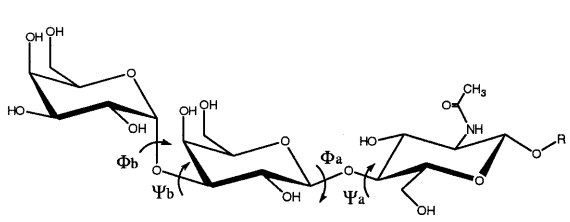

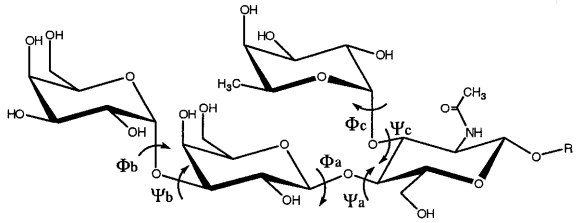

1 R: CH_3 **2** R: CH_2-CH_2-CH_2-NH_2 **3** R: CH_3 **4** R: CH_2-CH_2-CH_2-NH_2

Scheme 1. Schematic representation of oligosaccharides **1**–**4** with the labeling of the torsion angles of interest.

Table I. ^{1}H and ^{13}C[a] NMR data of a 6 mM solution of trisaccharide **2** in D_2O at 298°K.

Residue	1	2	3	4	5	6	6′
→4)β-GlcNAc(1→[b]							
δ_H	4.497	3.744	3.703	3.71	3.58	3.81	3.988
(Mult, $J_{x,x+1}$)	(d, 8)	(~t, l)			(dd, ls)	(dd, sl)	
δ_C	102.5	56.4	73.5	79.7	75.8	61.2	
→3)β-Gal*p*(1→							
δ_H	4.509	3.642	3.76	4.162	3.70	3.76?	3.76?
(Mult, $J_{x,x+1}$)	(d, 8)	(dd, ll)	(dd,ls)	(d,s)			
δ_C	104	70.7	78.5	66.0	76.5	62.2	
α-Gal*p*(1→							
δ_H	5.123	3.84	3.93	4.00	4.172	3.72	3.72
(Mult, $J_{x,x+1}$)	(d, 3.7)	(dd, sl)	(dd, ls)	(d, s)	(d, s)	(dd, sl)	
δ_C	96.7	69.6	70.4	70.4	72.2	62.2	

Key: multiplicity from phase-sensitive DQCOSY spectrum: l large, s small. Referenced to H1 of the α-Gal*p* residue in compound **1**.
[a]Internal reference (Hindsgaul *et al.*, 1982).
[b]^{1}H (^{13}C) data for the $OCH_2CH_2CH_2NH_2$ group: 3.690 and 3.993 (70.2), 1.92 m (27.6), 3.06 ~t (38.9); NAc CH_3: 2.02 s.

Table II. ^{1}H and ^{13}C[a] NMR data of a 8 mM solution of tetrasaccharide **4** in D_2O at 298K.

Residue	1	2	3	4	5	6	6′
→3,4)β-GlcNAc(1→[b]							
δ_H	4.504	3.93	3.843	3.94	3.578	3.844	3.992
(Mult, $J_{x,x+1}$)	(d, 8)	(dd, ll)				(dd, l, ~5)	(br d, l)
δ_C	101.9	56.8	75.8	74.0	75.6	61.0	
→3)β-Gal*p*(1→							
δ_H	4.504	3.572	3.756	4.14	3.56	3.722	3.722
(Mult, $J_{x,x+1}$)	(d, 8)	(dd, ll)		(d, 3.1)			
δ_C	103.65	70.5	78.4	65.8	75.6	62	
α-Gal*p*(1→							
δ_H	5.123	3.83	3.933	3.998	4.173	3.727	3.727
(Mult, $J_{x,x+1}$)	(d, ~ 4)	(dd, sl)	(dd, ls)		(~t, 7.8)		
δ_C	96.54	69.7	70	70	72.0	62.0	
α-Fuc*p*(1→							
δ_H	5.109	3.68	3.89	3.753	4.795	1.16	
(Mult, $J_{x,x+1}$)	(d, ~ 4.5)	(dd, sl)	(dd, ls)				
δ_C	99.68	68.78	70	73.5	67.70[a]	16.84	

Key: multiplicity from phase-sensitive DQCOSY spectrum: l large, s small.
[a]Internal reference (Hindsgaul *et al.*, 1982).
[b]^{1}H (^{13}C) data for the $OCH_2CH_2CH_2NH_2$ group: 3.690 and 3.993 (70.2), 1.92 m (27.6), 3.06 ~t (38.9); NAc CH_3: 2.02 s.

the N-acetyl substituent at the anomeric carbon; Li *et al.*, 1999). Partial proton data have been reported for compounds related to tetrasaccharide **3** and **4,** αGal1-3βGal1-4[αFuc1-3]βGlcNAc-OH; Joziasse *et al.*, 1993) and βGal1-4[αFuc1-3]βGlcNAc-OR

(where R = $-(CH_2)_8CO_2Me$; Hindsgaul *et al.*, 1982). The rotamer populations of the exocyclic groups of residues I and III of compounds **2** and **4** can be deduced from the fine structure of the H5/H6a,b crosspeaks (residue I, < 2 and ~ 5 Hz) and the $^3J_{H5,H6,6'}$ coupling constants (residue III, H5 – br t, 7.8 Hz), respectively. The former vicinal couplings (residue I) correspond to a 50/50 mixture of gg and gt populations, whereas the latter parameters (residue III) indicate a 50/50 mixture of tg and gt rotamers (Bock and Duus, 1994). Similar vicinal coupling constant data were reported for the αGal1-3βGal1-4βGlcNAc trisaccharide (Li *et al.*, 1999).

NOESY data. NOESY spectra were acquired for the trisaccharide **2** at 30 and 35°C with a 500-ms mixing time. Under these conditions the sign of the cross-peaks was opposite to those of the diagonal peaks (positive nOes, $\omega\tau_c < 1$). Inspection of the rows containing the $H1_{III}$ signal on the diagonal revealed interglycosidic crosspeaks with $H3_{II}$ and $H4_{II}$ in a 2:1 ratio in agreement with nOe data reported earlier for the related αGal1-3βGal1-4βGlcNAc trisaccharide (Li *et al.*, 1999).

At 5°C overall tumbling of compound **4** was slow enough to yield measurable crosspeak volumes with the same sign as the diagonal peaks (negative nOes, $\omega\tau_c > 1$) for all of the mixing times (100, 200, and 400 ms). However, at this temperature the anomeric signals displayed severe overlapping (α-sugars, $H1_{III}$ with $H1_{IV}$; β-sugars, $H1_I$ with $H1_{II}$) and summed cross-peak volumes have been considered in both cases. The corresponding nOe build-up curves were linear in keeping with the theoretical ones (*vide infra*). The experimental NOESY cross-peak volumes for both the anomeric protons and strategic protons with signals in nonoverlapping regions have been collected in Table III (bold) and will be discussed below. An expansion of the NOESY spectrum acquired with a 200-ms mixing time has been given in Figure 1.

Molecular dynamics simulations

Molecular dynamics trajectories of 3 ns were calculated for both oligosaccharides **1** and **3** in explicit water environment. During the simulation, trisaccharide **1** displays flexible behavior. Large ranges of the torsional angles are visited, specially for the Ψ angles of both glycosidic linkages (Figure 2). The history of torsion angles during the simulation have been superimposed on the energy maps of each linkage that were previously calculated using the MM3 program (Imberty *et al.*, 1995) (Figure 3). The βGal1-4GlcNAc linkage explores the large low-energy plateau characteristic of two pyranose rings linked in a equatorial-equatorial configuration (Pérez *et al.*, 2000). Variation ranges of 60° in Φ and 120° in Ψ centered on this plateau are observed that correspond approximately to an energy window of 4–5 kcal/mol when calculated using the MM3 software. The αGal1-3Gal linkage is more flexible, four discrete conformations are populated during the simulation, three of them being very different with respect to the Ψ angle. They correspond to the *trans*, *gauche*$^-$, and *gauche*$^+$ orientations of this torsion angle and have been labeled A, B, and C, respectively. Graphical representation of the lowest energy conformations of the trisaccharide are displayed in Figure 4. During the simulation, the trisaccharide starts from conformation B. After 500 ps, it makes short visits to conformation A, and after 1 ns stabilizes in this conformation during 200 ps. From there, it jumps for a single visit of 200 ps to conformation C, before returning to conformation B for the last ns. Another conformation, D, corresponds to a variation in the Φ angle and is visited only from conformation A.

The conformational behavior of the tetrasaccharide **3** is quite different. Branching of a fucose residue on position 3 of GlcNAc resulted in a drastic stiffening of the adjacent βGal1-4GlcNAc linkage. Because of the interactions between the Fuc and the βGal residues, the Lewis X moiety of the molecule exists as a unique conformational family corresponding to that observed by X-ray crystallography (Pérez *et al.*, 1996). As seen from Figures 2 and 3, the βGal1-4GlcNAc linkage conformation exhibits variations of no more than 30° around a conformation centered at Φ = –80° and Ψ = –120°. Although there is no direct interaction between the Fuc and the αGal residues, the αGal1-3Gal linkage flexibility is affected by the stiffening of the LacNAc backbone. The αGal1-3Gal is still flexible, but it adopts predominantly the B conformation (Figure 4) and makes only a short visit into the A region, with no stabilization in this area and no visit to the *gauche*$^-$ conformation. Due to the time scale of the simulation, it cannot be concluded that this particular conformation is not populated in solution. Nevertheless, it could be predicted that the presence of the fucose energetically favors the B conformers of the αGal1-3Gal linkage and reduces its flexibility.

Comparison of experimental and theoretical NMR data

Theoretical NOESY were calculated from the molecular dynamics simulations trajectories and compared with the experimental data. For the αGal-LacNAc trisaccharide, good agreement was obtained. The results do not differ significantly from those obtained by Li *et al.* (1999) and are therefore not presented further in this article. It could be confirmed that most of the flexibility of this molecule occurs from a conformational equilibrium between the two lowest-energy conformations at the αGal1-3Gal linkage (conformations A and B in Figure 4). Other conformations can also occur in solution, but their population is not significant.

Comparison of theoretical and experimental NOESY for the αGal-Lewis X is given in Table III. In general, the experimental NOESY volumes are smaller than the theoretical ones, a fact that can be explained by the rapid local motion of the methyl groups (NAc and Fucp). Because experimental and theoretical data have been obtained from tetrasaccharides **3** and **4**, respectively, small differences are observed at the anomeric center of the GlcNAc residue: the experimental volumes involving $H1_I$ are expected to be slightly different from the theoretical ones because a supplementary relaxation pathway exists for this spin via the protons of the $-CH_2CH_2CH_2NH_2$ pendant group.

There is an excellent agreement between modeled and solution conformations for the Lewis X moiety. The strong nOe observed between $H\text{-}5_{IV}$ and $H\text{-}2_{II}$ confirms the interaction between the two nonbonded residues αFuc and βGal. As for the flexible part of the tetrasaccharide, that is, the αGal1-3Gal linkage, no single conformation could explain the ensemble of NOESY data listed in Table III and represented in Figure 1. Of particular interest are the values of the $H\text{-}1_{III}/H\text{-}3_{II}$, $H\text{-}1_{III}/H\text{-}4_{II}$, and $H\text{-}5_{III}/H\text{-}3_{II}$ interactions because they are very sensitive to the conformational equilibrium of the αGal1-3Gal linkage. More precisely, conformation A of the tetrasaccharide is characterized by a short $H\text{-}1_{III}$ . . . $H\text{-}3_{II}$ distance, whereas conformation B displays a contact between $H\text{-}1_{III}$ and $H\text{-}4_{II}$

Table III. Comparison between experimental (bold) 500 MHz NOESY data of aqueous solution (T 5°C) of tetrasaccharide **4** with theoretical NOESY data obtained from molecular dynamics of tetrasaccharide **3**.

Diagonal protons	Off-diagonal protons	Relative theoretical and experimental (bold) cross-peak integrals for various τ_m (ms)		
		100	200	400
H1(I+II)	(H2+H4)I	0.020	0.037	0.059
		0.015	**0.030**	**0.053**
	H3I	0.009	0.018	0.029
		0.009	0.018	0.029
	H3II	0.012	0.021	0.030
		0.005	**0.010**	**0.017**
	H2II+H5(I+II)	0.035	0.061	0.094
		0.020	**0.033**	**0.058**
	OCH_2 subst at C1	*	*	*
		0.005	**0.010**	**0.014**
H4II	H5II	0.015	0.025	0.037
		0.015	0.025	0.037
	(H3+H6,6′)II	0.023	0.041	0.060
		0.022	**0.040**	**0.051**
	H1(III+IV)	0.024	0.042	0.063
		0.012	**0.023**	**0.036**
H1(III+IV)	H3II	0.009	0.015	0.024
		0.010	**0.025**	**0.047**
	H4II	0.024	0.042	0.063
		0.024	**0.032**	**0.060**
	H2III+H3I	0.028	0.050	0.082
		0.033	**0.051**	**0.104**
	H2IV	0.016	0.030	0.052
		0.016	0.030	0.052
	CH_3CO–	0.003	0.003	0.006
		0.004	**0.006**	**0.012**
H5III	H3II+H6,6′III	0.019	0.033	0.051
		0.033	**0.046**	**0.052**
	H3III	0.014	0.026	0.042
		0.014	0.026	0.042
	H4III	0.015	0.027	0.045
		0.058	**0.044**	**0.071**
H5IV	H1(I+II)	0.001	0.001	0.002
		0.003	ND	**0.005**
	H2II	0.011	0.019	0.029
		0.008	**0.021**	**0.038**
	H3IV	0.014	0.024	0.036
		0.014	0.024	0.036
	H4IV	0.015	0.026	0.039
		0.015	**0.027**	**0.045**
	MeIV	0.026	0.041	0.050
		0.006	**0.017**	**0.024**

Experimental data for interactions corresponding to fixed internuclear distances (underlined) were used as internal rulers.

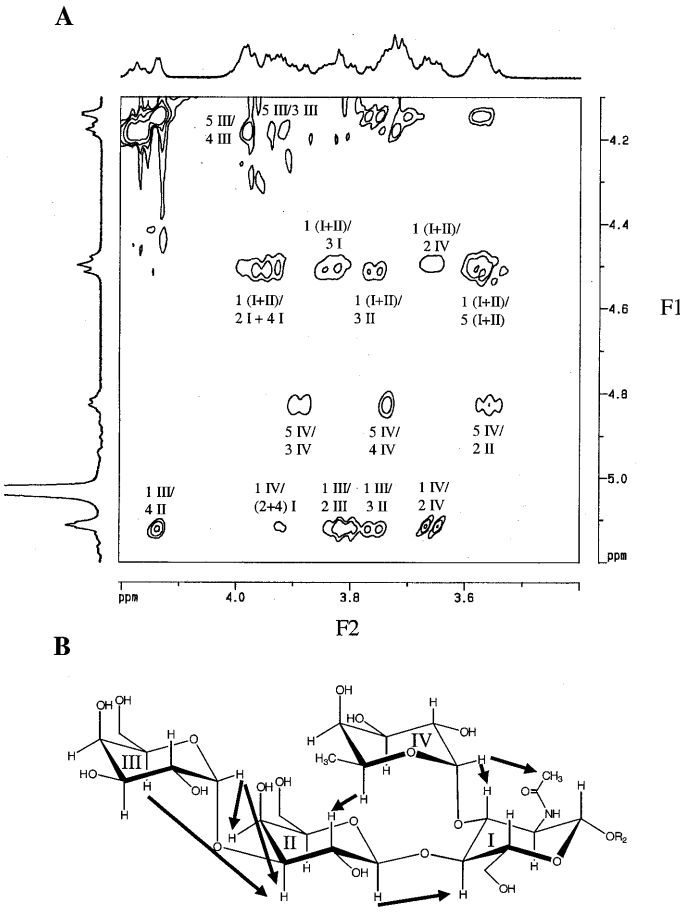

Fig. 1. An expansion of the NOESY spectrum of αGal-Lewis X (mixing time 200 ms, 5°C) with the low field signals on the diagonal (F1). Cross-peaks with the protons resonating at high field (F2) have been labeled (F1/F2). The observed inter-ring nOes effects are reported in Scheme 2.

(data not quantified in Table III due to overlapping signals). The simulation shown in Figures 2 and 3 where the αGal1-3Gal linkage is predicted to spend most of the time in conformation B while making several incursions of few tens of ps in energy minimum A allows for an excellent reproduction of these two experimentally observed NOESY values.

Discussion

The combination of experimental and theoretical approaches allowed for a precise determination of the effect of an additional fucose residue on the conformational behavior of the xenoantigen. This branched fucose strongly rigidifies the N-acetyllactosamine core but has a minor effect on the conformational behavior of the αGal1-3Gal linkage. Nevertheless, the B conformation, which is adopted by 60% of the population for the trisaccharide, seems to be even more favored for the tetrasaccharide. Interestingly, the B conformation is also the one that is observed ($\Phi = 56°$, $\Psi = 60°$) for the αGal1-3Gal linkage in the crystal structure of the blood group B trisaccharide (Otter *et al.*, 1999).

In conclusion, design of a rigid inhibitor that would mimic the antigenic conformation of the αGal1-3Gal epitope still represents a difficult problem. Due to the intrinsic flexibility of this linkage, it is difficult to predict the shape that will be recognized by an antibody. It is even possible that polyclonal antibodies may recognize different conformations of this molecule. Preformed xenoreactive antibodies are thought to arise during the first year of life, owing to stimulation of gut bacteria in the human host (Galili, 1993). It would be of special interest to identify the αGal epitope present in these bacterial polysaccharides and to determine the conformational epitopes that are responsible for the early immunological event.

In addition, there have been several examples of protein carbohydrate interactions where the "bioactive" conformation of the oligosaccharide ligand, that is, the one observed in the protein binding site, does not correspond to the most populated one in solution but rather to a secondary minimum (Imberty *et al.*, 1993; Imberty and Pérez, 2000). This has been exemplified recently in the crystal structures of E-selectin and P-selectin interaction with sialyl-Lewis X–containing ligand (Somers *et al.*, 2000). It was previously pointed that αGal-Lewis X shares some similarity to sialyl-LewisX (Joziasse *et al.*, 1993). The previous study demonstrates another similarity with the present one: both molecules consist of a semiflexible nonreducing end, borne by the rigid Lewis X moiety.

Materials and methods

Synthesis

Trisaccharide **2** was obtained as described previously (Pazynina *et al.*, 2001). Tetrasaccharide **4** was obtained by block synthesis 2 + 2 (see Scheme 2). Thioglycoside **8**, used as glycosyl-donor, was obtained by α-galactosylation of **6** by tetra-O-benzylbromogalactose **5** in the presence of silver triflate followed by reprotection giving rise to thioglycoside **7**. Glycosyl acceptor **12** was obtained by α-fucosylation of 4-OTr-substituted 1,6-anhydro-N-acetylglucosamine (Tyrtysh *et al.*, 2000) by tri-O-benzylfucopyranosylbromide under the conditions of the Lemieux reaction followed by removal of trityl protection. By reaction of thioglycoside **8** with glycosyl acceptor **12** in the presence of NIS and TflOH, tetrasaccharide **13** was obtained in a yield of 59%. Under conditions of deprotection and peracetylation, this tetrasaccharide was converted to tetrasaccharide **14** followed by acetolysis to open the anhydro cycle. The oxazoline obtained in the acetolysis reaction along with 1-αOAc-derivative were glycosylated with $HOCH_2CH_2CH_2NHCOCF_3$ without purification. Peracetate of tetrasaccharide **15** was isolated in a yield of 43%, and 27% of 1-OAc- and 13% 1-αOH-derivatives were obtained as by-products. Deprotection of compound **12** led to the desired tetrasaccharide **4**. The details of the synthesis will be published elsewhere.

NMR spectroscopy

Approximately 4 (3.5) mg of tetrasaccharide **4** (trisaccharide **2**), were lyophilized three times against D_2O to exchange the hydroxyl hydrogens, dissolved in 0.75 ml of 99.96% D_2O to afford a final concentration of ~8 mM (~6 mM), and then placed in a tube sealed under argon. NMR spectra were recorded on Varian 400 Inova (gHMQC and gHMBC), Varian 500 Unityplus (DQCOSY, total correlation spectroscopy [TOCSY] and NOESY) and a Bruker Avance 500 MHz (NOESY) spectrometers (double-resonance H/C gradient

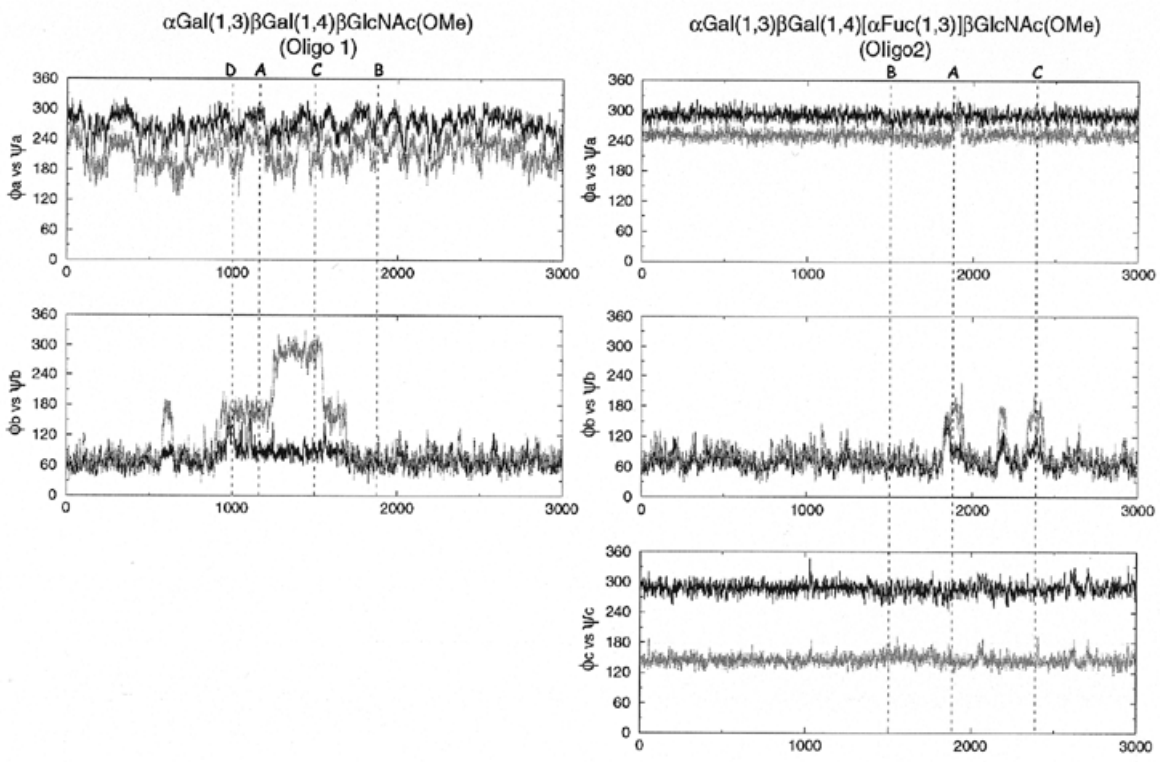

Fig. 2. Histories of the Φ and Ψ torsion angles of the glycosidic linkages of trisaccharide **1** and tetrasaccharide **3** during the 3-ns molecular dynamics simulation in water environment.

probe) at 25°C (COSYDQF, gHMQC, gHMBC, TOCSY). Regarding the 2D homonuclear and HMQC experiments, quadrature detection was achieved in the nonacquisition dimensions by the TPPI (Marion and Wüthrich, 1983) and the hypercomplex (States *et al.*, 1982) methods, respectively. Phase-shifted squared sinebell apodization functions were applied in both dimensions and the first points were scaled. Data were zero-filled to 4096 and 2048 points in F2 and F1, respectively. A polynomial baseline correction was applied in F2 after Fourier transformation.

In the case of the tetrasaccharide **4**, phase-sensitive NOESY experiments (Jeener *et al.*, 1979; Macura and Ernst, 1980) were recorded with mixing times of 100, 200, and 400 ms at 5°C, whereas for the trisaccharide **2** NOESY data were recorded with a mixing time of 500 ms at both 30 and 35°C. The cross-peak volumes were evaluated by comparison to a crosspeak volume for two protons separated by a fixed distance (underlined in Table III).

Nomenclature and starting models

Schematic representation of the oligosaccharides are given in Scheme 1 together with the labeling of the torsion angles of interest. These latter have been defined as follows: Φ = Θ(O-5′∇C-1′∇O-1′∇C-3) and Ψ = Θ(C-1′∇O-1′∇C-3—C-4) for the 1–3 linkages and Φ = Θ(O-5′∇C-1′∇O-1′∇C-4) and Ψ = Θ(C-1′∇O-1′∇C-4—C-5) for the 1–4 linkages. Starting 3D structures were built with the Sybyl program (SYBYL), using residues from the Monosaccharides Database (www.cermav.cnrs.fr/databank/monosaccharides) and orientations of glycosidic linkages corresponding to the energy minima reported on the MM3 energy map (Imberty *et al.*, 1995).

Simulation protocol

Simulations were performed using the AMBER-5.0 program package (Pearlman *et al.*, 1991) together with the GLYCAM-93 parameters for carbohydrates (Woods *et al.*, 1995). The molecules were hydrated in the Xleap module of AMBER by a periodic box of TIP3P waters, which was extended by 10 Å in each direction from the carbohydrate atoms and contained 1227 and 1291 water molecules for the tri- and tetrasaccharide, respectively. All simulations were run with the SANDER module of AMBER with SHAKE algorithm (Ryckaert *et al.*, 1977) (tolerance = 0.0005 Å) to constrain covalent bonds involving hydrogens, using periodic boundary conditions, a 2 fs time step, a temperature of 300°K with Berendsen temperature coupling (Berendsen *et al.*, 1984), a 9 Å cutoff applied to the Lennard-Jones interaction, and constant pressure of 1 atm. The nonbonded list was updated every 10 steps.

Equilibration was performed by first restraining the atoms of the oligosaccharide (water molecules were allowed to move) and running 1000 steps of minimization. After this initial minimization, all subsequent simulations were run by using the particle mesh Ewald method (Essmann *et al.*, 1995) within AMBER with a cubic B-spline interpolation order and a 10^{-6} tolerance for the direct space sum cutoff. The first step was followed by 25 ps of dynamics with the position of the oligosaccharide fixed. Equilibration was continued with 25 kcal/(mol. Å) restraints placed on all solute atoms, minimization for 1000 steps, followed by 3 ps of molecular dynamics, which allowed the water to relax around the solute. This equilibration was followed by five rounds of 600 steps of minimization where the solute restraints were reduced by 5 kcal/(mol. Å) during

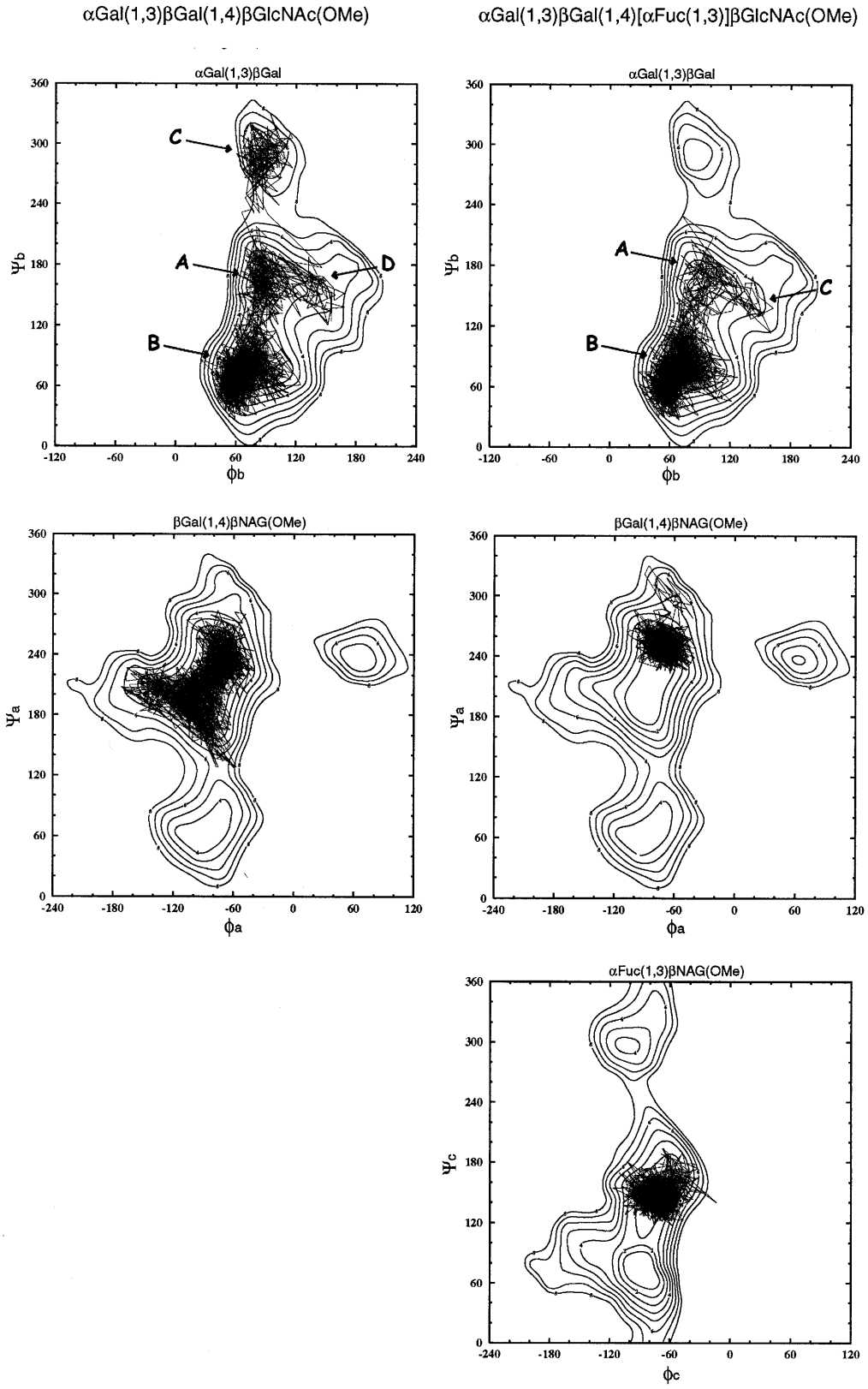

Fig. 3. Trajectories of the Φ and Ψ torsion angles of the glycosidic linkages of trisaccharide **1** and tetrasaccharide **3** during the 3-ns molecular dynamics simulation in water environment superimposed on the MM3 energy map of each of the corresponding disaccharides.

each round. Finally, the system was heated from 100 to 300°K over 2 ps and the production run was initiated. The molecular

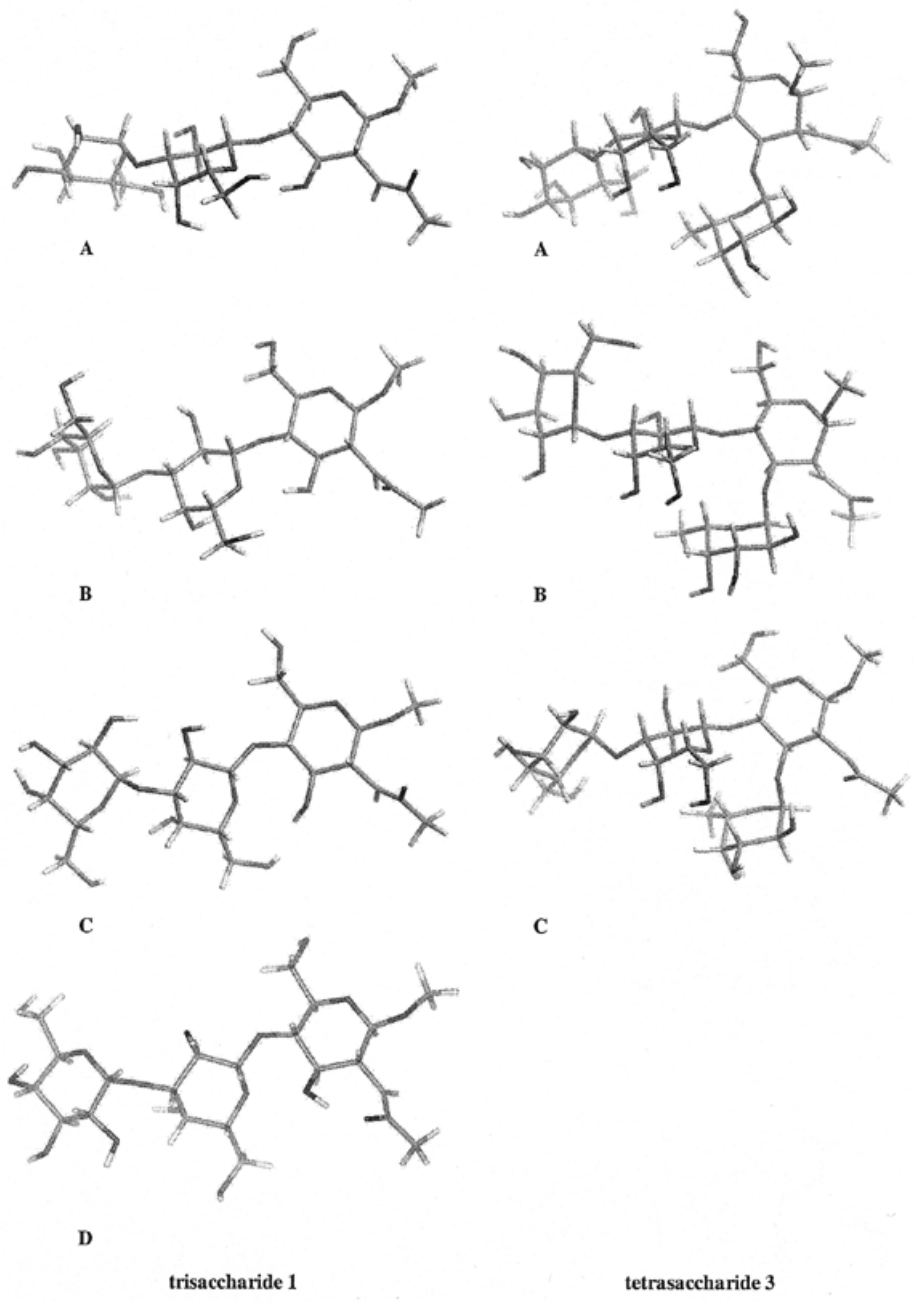

Fig. 4. Graphical representation of the main low-energy conformations of trisaccharide **1** and tetrasaccharide **3**.

dynamics trajectories were analyzed with the CARNAL module of AMBER.

Calculations of theoretical NMR data from molecular dynamics trajectories

Theoretical NOESY volumes were established from the averaged $\langle r^{-3} \rangle$ and $\langle r^{-6} \rangle$ interproton distance matrices of the molecular dynamics trajectories using the model-free approach of Lipari and Szabo (1982). This approach requires a precise description of Brownian motion including the nature (isotropic or anisotropic, etc.) and the characteristic rotational correlation time(s) and both the amplitude and correlation time for internal motion. Strictly speaking, this formalism is only valid when internal motions are not coupled to overall motion, which is likely not the case with small sugars. However, inspite of this limitation, the Lipari-Szabo spectral densities have been widely applied to small oligosaccharides. Motional models can be established from experimental NMR data but, due to the small amount of sample available acquisition times, would be unreasonably long; a strategy based on hydrodynamic theory was adopted. Inspection of molecular models with favorable orientations of the glycosidic linkages revealed a slightly anisotropic shape that included a longer axis of roughly 15 Å (17 Å when the van der Waals distance between the outer atoms and the solvent is

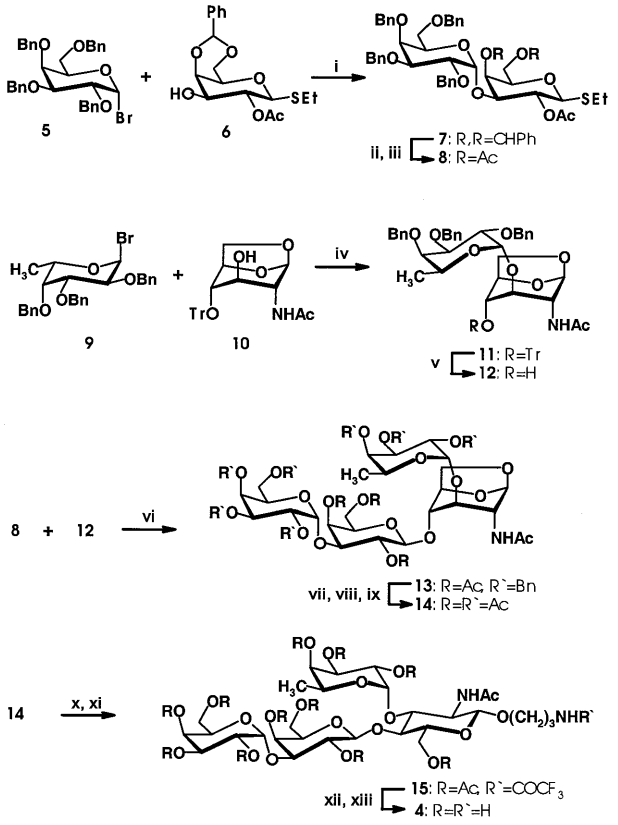

Scheme 2. Chemical synthesis of tetrasaccharide **4**.

taken into account) and a shorter axis of approximately 9 Å. When the axial ratio is less than 2 the influence on NOESY data is very small (<2–3%) (Ejchart *et al.*, 1992) so that the most simple isotropic model corresponding to a sphere of radius 7–8 Å was expected to be suitable for the tetrasaccharide **4**. The rotational correlation time for a spherical molecule with a radius of 7.5 Å was established to be 0.86 ns from the molecular volume with the Stokes-Einstein-Debye relation as follows:

$$\tau_c = 4\,\pi\,a^3\,\eta_0 / 3\,k\,T$$

where a is the molecular radius, η_0 the viscosity of the solvent (Matsunga and Nagashima, 1983), k the Boltzmann constant, and T the absolute temperature. This theoretical τ_c value was adjusted to 0.88 ns to best fit the experimental data while using a correlation time of 50 ps (τ_e) for internal motion. Three different values for the amplitude of internal motion (characterized by the order parameter S^2_{ang}, which varies from 1.0 for a rigid molecule to 0 for a totally flexible one) were implemented in the calculations corresponding to (1) 0.9 for the methine/methine interactions of the nonterminal sugars, I and II; (2) 0.85 for the interactions of the terminal sugars, III and IV; and (3) 0.7 for the interactions involving the pendant $-CH_2OH$ and $-CH_3$ groups.

Acknowledgments

E.B. was accorded a grant by the Xenotranplantation Project BIO4CT972242 of the Biotech program from European Union. The stay of F.C. in Grenoble was supported by Ministerio de Educación y Cultura. The authors are endebted to Drs. D. Bouhours and J.F. Bouhours (Nantes) for helpful discussion. T.T. was supported by Syntesome GmbH (Munich, Germany).

Abbreviations

gHMBc; gHMQC; COSYDQF; DQCOSY; NMR, nuclear magnetic resonance; NOESY, nuclear Overhauser effect spectroscopy; TOCSY, total correlation spectroscopy;

References

Auchincloss, H.J. and Sachs, D.H. (1998) Xenogeneic transplantation. *Annu. Rev. Immunol.*, **16**, 433–470.

Berendsen, H.J.C., Postma, J.P.M., and van Gunsteren, W.V. (1984) Molecular dynamics with coupling to an external bath. *J. Chem. Phys.*, **81**, 3684–3690.

Bizik, F. and Tvaroska, I. (1995) Conformational analysis of disaccharide fragments of blood group determinants in solution by molecular modelling. *Chem. Papers*, **49**, 202–214.

Bock, K. and Duus, J.O. (1994) A conformational study of hydroxymethyl groups in carbohydrates investigated by ^{1}H NMR spectroscopy. *J. Carbohydr. Chem.*, **13**, 513–543.

Bouhours, D., Liaigre, J., Lemoine, J., Mayer-Posner, F., and Bouhours, J.F. (1998) Two novel isoneolacto-undecaglycosylceramides carrying Galα1–>3Lewis^x on the 6-linked antenna and N-acetylneuraminic acid α2–>3 or Galactose α1–>3 on the 3-linked antenna, expressed in porcine kidney. *Glycoconj. J.*, **15**, 1001–1016.

Bouhours, D., Liaigre, J., Naulet, J., Maume, D., and Bouhours, J.F. (1997) A novel glycosphingolipid expressed in pig kidney: Galα1–3Lewis(x) hexaglycosylceramide. *Glycoconj. J.*, **14**, 29–38.

Cascalho, M. and Platt, J.L. (2001) The immunological barrier to xeno-transplantation. *Immunity*, **14**, 437–446.

Cooper, D.K., Good, A.H., Koren, E., Oriol, R., Malcolm, A.J., Ippolito, R.M., Neethling, F.A., Ye, Y., Romano, E., and Zuhdi, N. (1993) Identification of alpha-galactosyl and other carbohydrate epitopes that are bound by human anti-pig antibodies: relevance to discordant xenografting in man. *Transpl. Immunol.*, **1**, 198–205.

Ejchart, A., Dabrowski, J., and von der Lieth, C.W. (1992) Solution conformation of mono- and difucosyllactoses as revealed by rotating-frame NOE-based mapping and molecular mechanics and molecular dynamics calculations. *Magn. Res. Chem.*, **30**, S105–S114.

Essmann, U., Perera, L., Berkowitz, M.L., Darden, T., Lee, H., and Pedersen, L.G.J. (1995) A smooth particle mesh ewald method. *Chem. Phys.*, **103**, 8577–8593.

Galili, U. (1993) Interaction of the natural anti-Gal antibody with α-galactosyl epitopes: a major obstacle for xenotransplantation in humans. *Immunol. Today*, **14**, 480–482.

Galili, U., Clark, M.R., Shohet, S.B., Buehler, J., and Macher, B.A. (1987) Evolutionary relationship between the natural anti-Gal antibody and the Gal alpha 1—3Gal epitope in primates. *Proc. Natl Acad. Sci. USA*, **84**, 1369–1373.

Galili, U., Shohet, S.B., Kobrin, E., Stults, C.L., and Macher, B.A. (1988) Man, apes, and Old World monkeys differ from other mammals in the expression of alpha-galactosyl epitopes on nucleated cells. *J. Biol. Chem.*, **263**, 17755–17762.

Hindsgaul, O., Norberg, T., Le Pendu, J., and Lemieux, R.U. (1982) Synthesis of type 2 human blood-group antigen determinants. The H, X, and Y haptens and variations of the H type 2 determinants of probes for the combining site of the lectin I of *Ulex europaeus*. *Carbohydr. Res.*, **109**, 109–142.

Imberty, A. and Pérez, S. (2000) *Structure*, conformation and dynamics of bioactive oligosaccharides: theoretical approaches and experimental validations. *Chem. Rev.*, **100**, 4567–4588.

Imberty, A., Bourne, Y., Cambillau, C., Rougé, P., and Pérez, S. (1993) Oligosaccharide conformation in protein-carbohydrate complexes. *Adv. Biophys. Chem.*, **3**, 71–118.

Imberty, A., Mikros, E., Koca, J., Mollicone, R., Oriol, R., and Pérez, S. (1995) Computer simulation of histo-blood group oligosaccharides. Energy maps of all constituting disaccharides and potential energy surfaces of 14 ABH and Lewis carbohydrate antigens. *Glycoconj. J.*, **12**, 331–349.

Jeener, J., Meier, B.H., Bachmann, P., and Ernst, R.R. (1979) Investigation of exchange processes by two-dimensional NMR spectroscopy. *J. Chem. Phys.*, **71**, 4546–4553.

Joziasse, D.H., Schiphorst, W.E., Koeleman, C.A., and Van den Eijnden, D.H. (1993) Enzymatic synthesis of the alpha 3-galactosyl-Lex tetrasaccharide: a potential ligand for selectin-type adhesion molecules. *Biochem. Biophys. Res. Commun.*, **194**, 358–367.

Lemieux, R.U., Bock, K., Delbaere, L.T.J., Koto, S., and Rao, V.S.R. (1980) The conformations of oligosaccharides related to the ABH and Lewis human blood group determinants. *Can. J. Chem.*, **58**, 631–653.

Li, J., Ksebati, M.B., Zhang, W., Guo, Z., Wang, J., Yu, L., Fang, J., and Wang, P.G. (1999) Conformational analysis of an α-galactosyl trisaccharide epitope involved in hyperacute rejection upon xenotransplantation. *Carbohydr. Res.*, **315**, 76–88.

Lipari, G. and Szabo, A. (1982) Model-free approach to the interpretation of Nuclear Magnetic Resonance relaxation in macromolecules. 1. Theory and range of validity. *J. Am. Chem. Soc.*, **104**, 4546–4559.

Macura, S. and Ernst, R.R. (1980) Elucidation of cross relaxation in liquids by two-dimensional NMR spectroscopy. *Mol. Phys.*, **41**, 95–117.

Marion, D. and Wüthrich, K. (1983) Application of phase sensitive two-dimensional correlated spectroscopy (COSY) for measurements of 1H-1H spin-spin coupling constants in proteins. *Biochem. Biophys. Res. Commun.*, **113**, 967–974.

Matsunga, N. and Nagashima, A. (1983) Transport of liquid and gazeous D_2O over a wide range of temperature and pressure. *J. Phys. Chem. Ref. Data*, **12**, 933–966.

Oriol, R., Candelier, J.J., Taniguchi, S., Balanzino, L., Peters, L., Niekrasz, M., Hammer, C., and Cooper, D.K.C. (1999) Major carbohydrate epitopes in tissues of domestic and African wild animals of potential interest for xenotransplantation research. *Xenotransplantation*, **6**, 78–89.

Otter, A., Lemieux, R.U., Ball, R.G., Venot, A.P., Hindsgaul, O., and Bundle, D.R. (1999) Crystal state and solution conformation of the B blood group trisaccharide α-L-Fuc*p*-(1–2)-[α-D-Gal*p*-(1–3)]-β-D-Gal*p*-OCH3. *Eur. J. Biochem.*, **259**, 295–303.

Pazynina, G.V., Tyrtysh, T.V., and Bovin, N.V. (2001) Synthesis of histo blood-group antigens A and B (type 2), xenoantigen Galα1-3Galβ1-4GlcNAc, and related type 2 backbone oligosaccharides in spacered form. *Carbohydr. Lett.*, in press.

Pearlman, D.A., Case, D.A., Caldwell, J.C., Seibel, G.L., Singh, C.U., Weiner, P., and Kollman, P.A. (1991) AMBER. San Franscico, CA, University of California.

Pérez, S., Gautier, C., and Imberty, A. (2000). Oligosaccharide conformations by diffraction methods. In B. Ernst, G. Hart, P. Sinay (eds.), *Oligosaccharides in chemistry and biology: a comprehensive handbook*. Wiley/VCH, Weinheim, pp. 969–1001.

Pérez, S., Mouhous-Riou, N., Nifant'ev, N.E., Tsvetkov, Y.E., Bachet, B., and Imberty, A. (1996) Crystal and molecular structure of a histo-blood group antigen involved in cell adhesion: the Lewis X trisaccharide. *Glycobiology*, **6**, 537–542.

Ryckaert, J.P., Cicotti, G., and Berendsen, H.J.C. (1977) Numerical integration of the cartesian equations of motion of a system with constraints: molecular dynamics of n-alkanes. *J. Comp. Phys.*, **23**, 327–341.

Samuelsson, B.E., Rydberg, L., Breimer, M.E., Backer, A., Gustavsson, M., Holgersson, J., Karlsson, E., Uyterwaal, A.C., Cairns, T., and Welsh, K. (1994) Natural antibodies and human xenotransplantation. *Immunol. Rev.*, **141**, 151–168.

Sandrin, M.S., Vaughan, H.A., Dabkowski, P.L., and McKenzie, I.F. (1993) Anti-pig IgM antibodies in human serum react predominantly with Gal(alpha 1–3)Gal epitopes. *Proc. Natl Acad. Sci. USA*, **90**, 11391–11395.

Somers, W.S., Tang, J., Shaw, G.D., and Camphausen, R.T. (2000) Insights into the molecular basis of leukocyte tethering and rolling revealed by structures of P- and E-selectin bound to SLe^x and PSGL-1. *Cell*, **103**, 467–479.

States, D.J., Haberkorn, R.A., and Ruben, D.J. (1982) A two-dimensional nuclear Overhauser experiment wtih pure absorption phase in four quadrants. *J. Magn. Reson.*, **48**, 286–292.

Strotz, C.A. and Cerezo, A.S. (1994) Use of a general purpose force-field (MM2) for the conformational analysis of the disaccharide α-D-galacto-pyranosyl-(1–3)-β-D-galactopyranose. *J. Carbohydr. Chem.*, **13**, 235–247.

Tyrtysh, T.V., Byramova, N.E., and Bovin., N.V. (2000) 1, 6-Anhydro-N-acetyl-β-D-glucosamine in the oligosaccharide synthesis: I. Synthesis of 3-acetate and 3-benzoate of 1, 6-anhydro-N-acetyl-β-D-glucosamine via the 4-O-trityl derivative. *Russ. J. Bioorgan. Chem.*, **26**, 414–418.

Woods, R.J., Dwek, R.A., Edge, C.J., and Fraser-Reid, B. (1995) Molecular mechanical and molecular dynamical simulations of glycoproteins and oligosaccharides. 1. GLYCAM_93 parameter development. *J. Phys. Chem.*, **99**, 3832–3846.